# Density Functional Analysis of Copper Doping Effects on the OER Activity of Nickel-Iron Phosphate

Rizky Dio Idhola<sup>1,2</sup>, Ahmad Nuruddin <sup>1,3,4</sup>, Adhitya Gandaryus Saputro <sup>1,3,4,\*</sup>

<sup>1</sup> Graduate Program of Engineering Physics, Faculty of Industrial Technology, Institut Teknologi Bandung, Bandung, West Java 40132, Indonesia
<sup>2</sup> PT PLN (Persero), Indonesia

**Abstract.** This study explores the impact of Cu doping on the oxygen evolution reaction (OER) activity of bimetallic NiFe phosphate using density functional theory-based calculations. The results indicate that Cu doping improves the catalytic performance at the Fe site by lowering the overpotential, while slightly increasing it at the Ni site. The Cu site, however, shows poor OER activity due to weak intermediate binding.

**Keywords:** Cu doping; Density functional theory; NiFe Phosphate; Oxygen evolution reaction.

#### 1 Introduction

Hydrogen is a crucial energy carrier and storage medium for the global energy transition, but it must be extracted from compounds like water [1-3]. Among hydrogen production methods, water electrolysis is promising for its ability to produce high-purity hydrogen [4]. However, the oxygen evolution reaction (OER) at the anode limits the efficiency of this process, making the development of effective OER catalysts essential [5]. While noble metal-based catalysts like iridium (Ir) are highly effective, their high cost and scarcity hinder large-scale applications, highlighting the need for more affordable and abundant alternatives [6].

Nickel phosphate and bimetallic nickel phosphate have recently emerged as promising candidates for oxygen evolution reaction (OER) applications, thanks to their favorable catalytic properties [7], [8]. Our prior research, which combined experimental and computational approaches, has demonstrated that alloying nickel phosphate with transition metals such as manganese (Mn), iron (Fe), and cobalt (Co) in a 1:1 ratio significantly enhances OER activity. Among these, the NiFe phosphate system exhibited the best performance [9]. However, there is still

Received \_\_\_\_\_\_, Revised \_\_\_\_\_, Accepted for publication \_\_\_\_\_ Copyright © xxxx Published by ITB Journal Publisher, ISSN: xxxx-xxxx, DOI: 10.5614/xxxx

<sup>&</sup>lt;sup>3</sup> Quantum and Nano Technology Research Group, Faculty of Industrial Technology, Institut Teknologi Bandung, 40132 Bandung, Indonesia

<sup>&</sup>lt;sup>4</sup> Research Centre for Nanoscience and Nanotechnology, Institut Teknologi Bandung, Bandung, West Java 40132, Indonesia \*Email: gandaryus@itb.ac.id

room for improvement in NiFe phosphate's performance, particularly due to the limitations of the Fe site, which binds OER intermediates more strongly than the Ni site, resulting in higher overpotential.

To address this, we propose modifying the NiFe phosphate catalyst by introducing copper (Cu) doping. Copper, known for its more negative d-band center compared to both nickel and iron, could weaken the interaction between OER intermediates and the Fe site, potentially reducing the overpotential [10]. This surface engineering approach aims to shift the OER overpotential at both Ni and Fe sites, thereby improving the overall catalytic performance. In this study, we investigate the OER activity of Cu-doped NiFe phosphate using density functional theory (DFT) calculations to evaluate the effect of Cu doping on the OER overpotential and provide insights into the enhanced catalytic behavior of the doped system.

# 2 Methodology

Quantum Espresso was used to do all DFT computations [11]. Ultrasoft pseudopotentials were used to simulate the atoms core electrons [12]. The Perdew-Burke-Ernzerhof (PBE) functional is used in the extended gradient approximation to represent exchange and correlation effects. Van der Waals corrections were also included in the energy calculations, and Grimme's semi-empirical D2 approach was used [13].

We employ a  $2 \times 1$  NiFePO(100) facet, which has the lowest surface energy as reported in our earlier work [9], to represent the surface active site. In Figure 1, the unit cell's size is displayed. The top layer was allowed to relax throughout the optimization, while the bottom two layers were fixed to reflect the bulk state. As per our earlier research, because of the high unit cell size, integration in the Brillouin zone was only carried out at the gamma point [9]. A density cutoff of 500 Ry and a kinetic energy cutoff of 50 Ry were used. In the normal direction of the surface, a 15 Å vacuum was introduced to prevent interactions between periodic boundaries. Dipole adjustments for surface supercell calculations were also investigated [14]. We relaxed the systems until the remaining force on each atom was less than 0.025 eV/Å. Calculations for isolated molecules were performed in a 30 Å x 30 Å cubic cell located near the gamma point.

We assume that the Cu dopant will substitute the Ni atom on the NiFePO(100) surface since it gives the lowest total energy. The stability of the substitution of a surface Ni atom by Cu dopant is checked by calculating the formation energy  $(E_{form})$ :

$$E_{form} = E_{\text{NiFePO;Ni} \to \text{Cu}} - (E_{NiFePO} - \mu_{Ni} + \mu_{\text{Cu}})$$
 (1)

Where  $E_{\text{NiFePO;Ni}\rightarrow\text{Cu}}$  is the energy of the NiFePO(100) surface doped by a Cu atom,  $E_{NiFePO}$  energy of pristine NiFePO(100) surface, and  $\mu$  the chemical potential of the element. This calculation gives a negative  $E_{\text{form}}$ , indicating a stable dopant formation. The unit cell model for NiFePO(100)-Cu surface is presented in Figure 1.

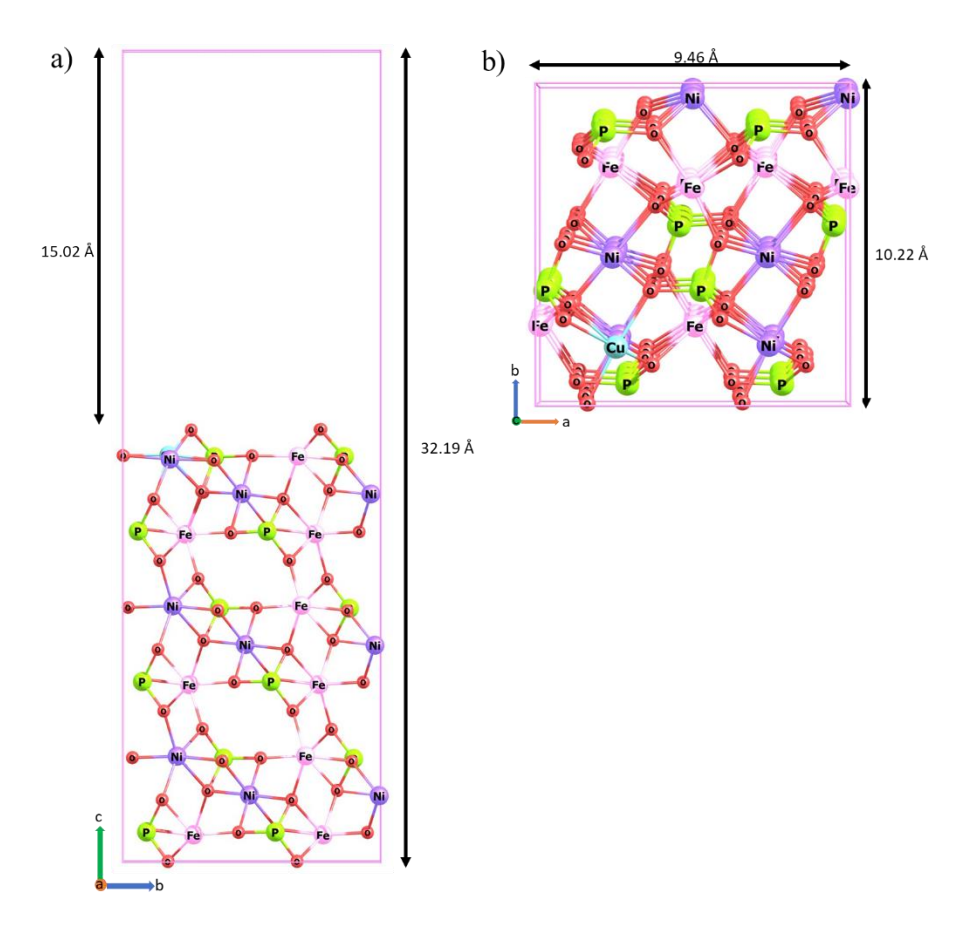


**Figure 1** Unit cell model of the most stable NiFePO(100) surface-Cu. (a) Side view and (b) top view.

The adsorption energy ( $E_{ads}$ ) of an OER intermediate on NiFePO(100)-Cu surface is calculated by the following formula[15]:

$$E_{\text{ads}} = E_{\text{NiFePO-Cu+mol}} - (E_{\text{NiFePO-Cu}} + E_{\text{mol}})$$
 (2)

where,  $E_{\rm NiFePO-Cu+mol}$ ,  $E_{\rm NiFePO-Cu}$ , and  $E_{\rm mol}$  are the total energies of an adsorbed OER intermediate on the NiFePO(100)-Cu surface, clean NiFePO(100)-Cu surface, and an isolated OER intermediate, respectively.

The thermodynamic performance of NiFePO(100)-Cu was evaluated utilizing the Gibbs free energy profile. Using the computational hydrogen electrode (CHE) approach [16], we calculated the change in free energy for each OER phase involving proton/electron transfer. This technique approximates the Gibbs free energy of  $[H^+ + e^-]$  using the energy of  $\frac{1}{2}H_2$  in the gas phase at standard conditions (pH = 0,  $p_{H2}$  = 1 bar, and T = 298.15 K). The change in Gibbs free energy of the electrochemical reaction in OER (\*AH  $\rightarrow$  \*A + H<sup>+</sup> +  $e^-(U)$ ) with respect to potential bias U can be calculated as:

$$\Delta G(U) = E(*A) - E(*AH) + 0.5E(H_2) + \Delta ZPE - T\Delta S + pH k_BT ln 10 - eU$$
 (3)

where E(\*A) and E(\*AH) represent the energies of the adsorbed \*A and \*AH species obtained from DFT calculations.  $\Delta$ ZPE and  $\Delta$ S represent zero-point energy and entropy changes, respectively.

To assess the thermodynamic performance of each active site in the OER, we look at the overpotential obtained from the Gibbs free energy profile. The overpotential at equilibrium potential is calculated as  $\eta = \Delta G_{max}^{equilibrium}$ /e. Here,  $\Delta G_{max}^{equilibrium}$  refers to the greatest Gibbs free energy change at any of the four OER phases, whereas e represents the total electron charge associated with the elementary step with the highest  $\Delta G$ [15].

## 3 Result and discussion

OER mechanism normally occurs through the following elementary steps:

$$* + H_2O_{(1)} \rightarrow *H_2O$$
 (4)

$$H_2O^* \to OH^* + H^+ + e^-$$
 (5)

$$OH^* \to O^* + H^+ + e^-$$
 (6)

$$O^* + H_2O \rightarrow OOH^* + H^+ + e^-$$
 (7)

$$OOH^* \rightarrow ^* + O_2 + H^+ + e^-$$
 (8)

The geometries of OER intermediates adsorptions on the Ni, Fe, and Cu active sites of NiFePO(100)-Cu surface, their adsorption energies, Gibss free energy profiles, and OER overpotential are given in Figure 2, Table 1, Figure 3 and Table 2, respectively.

From Figure 2 and Table 1, it is clear that the OER intermediates, including \*OH, \*O, and \*OOH, can generally be stabilized at the transition metal sites of the NiFePO(100)-Cu surface. These intermediates tend to follow similar adsorption modes across the various active sites, implying that the surface structure and chemical environment provided by the NiFePO(100)-Cu catalyst offer suitable bonding conditions for OER. However, as revealed by the data in Table 1, the strength of intermediate adsorption differs depending on the type of transition metal (Fe, Ni, or Cu) present at the active sites. Specifically, the adsorption energy of the intermediates follows the order Fe > Ni > Cu. This trend indicates that Fe exhibits the strongest interaction with the OER intermediates, followed by Ni, with Cu displaying the weakest binding affinity.

The variation in adsorption energy is crucial because it directly influences the reaction pathway and the overpotential required for the OER at each active site. Stronger adsorption of intermediates typically leads to a lower overpotential, as it facilitates the progression of the reaction steps. However, overly strong adsorption can also hinder the release of intermediates, potentially slowing down the overall catalytic cycle. On the other hand, weaker adsorption may reduce the catalyst's ability to effectively bind intermediates, leading to a higher overpotential and poorer catalytic performance.

**Table 1** Adsorption energies of OER intermediates on NiFePO(100)-Cu surfaces

Surface	Adsorption Site	$E_{ads}^{H_2O*}$ (eV )	E <sup>OH*</sup> (eV )	<i>E</i> <sub>ads</sub> (eV )
	Fe	-1.32	-1.93	-0.72
NiFePO(100)-Cu	Ni	-1.25	-1.18	0.03
	Cu	-0.97	-1.00	0.88

Adsorption Site	$H_2O$	ОН	0	ООН
Fe		Te a	Fe On	
Ni				
Cu		P		

**Table 2** Geometries of  $H_2O$ , OH, O, and OOH intermediates adsorptions on the active sites of NiFePO(100)-Cu surface

Table 2 further illustrates the effect of Cu doping on the overpotential of the Ni and Fe active sites. Although the magnitude of the shift is not large, it is noticeable that the inclusion of Cu has a tangible impact on the overpotential. Specifically, the overpotential at the Fe site is reduced by 0.03 V, which represents an improvement in OER performance. Conversely, the overpotential at the Ni site increases slightly by 0.01 V. This suggests that Cu doping modifies the d-band center of both Fe and Ni sites, leading to a shift in their overpotential values. Unfortunately, the overpotential at the Cu site remains quite high, at 1.00 V, which indicates suboptimal OER activity at that site. Nonetheless, the overpotentials at the Ni and Fe sites remain superior to that of the benchmark IrO<sub>2</sub> catalyst.

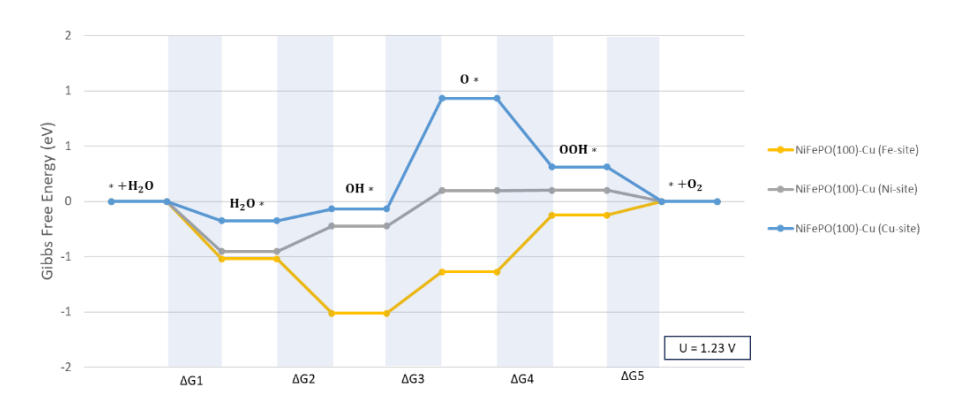


Figure 2 OER free energy profile of NiFePO(100)-Cu surface

TDS Active site η (V) 0.54 4 NiFePO(100) @Fe [9] NiFePO(100) @Ni [9] 0.31 4 NiFePO(100)-Cu @Fe 0.51 NiFePO(100)-Cu @Ni 0.32 3 NiFePO(100)-Cu @Cu 1.00 3 0.56 IrO<sub>2</sub> [17]

 Table 3
 OER overpotential of NiFePO(100)-Cu surface

The poor OER performance at the Cu site can be attributed to its weaker binding affinity for OER intermediates compared to the Fe and Ni sites. This is due to the fact that the d-band center of Cu is generally further from the Fermi level than that of Fe and Ni [10], resulting in less effective stabilization of the OER intermediates. Based on this understanding, we hypothesize that further reduction in the OER overpotential could be achieved by doping with transition metals that possess a more positive d-band center than Cu, such as Mn or Co. These metals may facilitate stronger interactions with OER intermediates, potentially lowering the overpotential and enhancing overall catalytic performance.

# 4 Conclusion

In this study, we investigated the OER activity on a Cu-doped NiFe phosphate surface using density functional theory-based calculations. The results reveal that Fe exhibits the strongest interaction with OER intermediates, followed by Ni, with Cu showing the weakest binding. This variation in adsorption energies significantly affects the overpotential at each active site. Cu doping reduces the overpotential at the Fe site by 0.03 V, enhancing catalytic activity, while slightly increasing the overpotential at the Ni site by 0.01 V. The Cu site, however, demonstrates poor OER performance, with a high overpotential of 1.00 V. Nevertheless, the Fe and Ni sites show better performance than the benchmark IrO<sub>2</sub> catalyst. These findings suggest that doping with other transition metals with a more positive *d*-band center, such as Mn or Co, could further improve OER performance by lowering overpotential and enhancing intermediate adsorption.

### Acknowledgement

We acknowledge the research fund granted by Institut Teknologi Bandung, under grant scheme "Riset Unggulan ITB". This work also supported by PT PLN (Persero), under "Pendidikan Formal Jarak Jauh Kerjasama PLN - ITB" programme. Some of the calculations were performed using the HPC facility at the Research Center for Nanosciences and Nanotechnology (RCNN), Institut Teknologi Bandung.

### References

- [1] Li, Y. & Zhao, C., *Iron-Doped Nickel Phosphate as Synergistic Electrocatalyst for Water Oxidation*, Chemistry of Materials, **28**(16), pp. 5659–5666, Aug. 2016.
- [2] Squadrito, G. et al., The green hydrogen revolution, Renew Energy, **216**(119401), Nov. 2023.
- [3] Malik, F. R. et al., Overview of hydrogen production technologies for fuel cell utilization, Elsevier B.V., 2023.
- [4] Khan, N. A. et al., Effective CuO/CuS heterostructures catalyst for OER performances, Int J Hydrogen Energy, **48**(80), pp. 31142–31151, Sep. 2023.
- [5] Wang L. et al., Interface engineering of porous nickel-iron phosphates with enriched oxygen vacancies as an efficient bifunctional electrocatalyst for high current water splitting, Electrochim Acta, 443(141932), Mar. 2023.
- [6] Xing, J. et al., Electro-synthesis of 3D porous hierarchical Ni-Fe phosphate film/Ni foam as a high-efficiency bifunctional electrocatalyst for overall water splitting, J Mater Chem A Mater, 4(36), pp. 13866–13873, Agu. 2016.
- [7] Septiani, N. L. W. et al., Tailorable nanoarchitecturing of bimetallic nickel—cobalt hydrogen phosphate via the self-weaving of nanotubes for efficient oxygen evolution, J. Mater. Chem. A, 8(6), pp. 3035–3047, Jan. 2020.
- [8] Qian, L., & Miao, Y., Nanosheet organized flower-like Co/Zn phosphate on nickel foam for efficient water splitting in both acid and basic solutions, Polyhedron, **160**(28), pp. 213–218, Jan. 2019.
- [9] Nuruzzahran, M. A. et al., Oxygen Evolution Reaction Activity of  $Ni_3(PO_4)_2$  and Bimetallic  $Ni_3M_3(PO_4)_4$  (M = Mn, Fe, Co): Insights from DFT and Experimental Validation, submitted for publication.
- [10] Vojvodic, A. et al., Electronic Structure Effects in Transition Metal Surface Chemistry, Top Catal, **57**(1), pp. 25–32, Nov. 2014.

- [11] Giannozzi, P. et al., QUANTUM ESPRESSO: a modular and open-source software project for quantum simulations of materials, Journal of Physics: Condensed Matter, **21**(39), pp. 395502, Sep. 2009.
- [12] Vanderbilt, D., Soft self-consistent pseudopotentials in a generalized eigenvalue formalism, Phys Rev B, **41**(11), pp. 7892–7895, Apr. 1990.
- [13] Grimme, S., Semiempirical GGA-type density functional constructed with a long-range dispersion correction, J Comput Chem, **27**(15), pp. 1787–1799, Nov. 2006.
- [14] Bengtsson, L., *Dipole correction for surface supercell calculations*, Phys Rev B, **59**(19), pp. 12301–12304, May 1999.
- [15] Sholl, D. S., & Steckel, J. A., *Density functional theory: a practical introduction*, John Wiley & Sons, 2022.
- [16] Nørskov, J. K. et al., Origin of the overpotential for oxygen reduction at a fuel-cell cathode, Journal of Physical Chemistry B, 108(46), pp. 17886– 17892, Nov. 2004.
- [17] Rossmeisl, J. et al., Electrolysis of water on oxide surfaces, Journal of Electroanalytical Chemistry, **607**(1–2), pp. 83–89, Sep. 2007.